The Crack Path Evolution for Monotonic and Cyclic Loading

K. P. Mróz and Z. Mróz

Institute of Fundamental Technological Research, Polish Academy of Sciences,
Warsaw, ul. 5b Pawińskiego St.,
kmroz@ippt.gov.pl and zmroz@ippt.gov.pl

ABSTRACT.
The models of crack growth in mixed mode conditions are reviewed for the plane(2D) and three-dimensional (3D) states of stress. Both critical load value and crack path or surface growth are predicted by different criteria in terms of elastic singular stress states and T-stress component. Both monotonic and cyclic loading are considered. The concepts of smooth and rough crack surface are discussed with application to 3D crack surface growth.

INTRODUCTION

The prediction of crack growth path under imposed loading and of its rate of growth constitutes most important problem in fracture mechanics. The present paper will apply LEFM to predict crack growth but the effects of plasticity and damage will be accounted for by postulating the relevant fracture criteria. The crack growth can be simulated as a succession of straight segment in plane cases or linear surface elements in 3-D cases. The effects of crack curvature can also be incorporated in the analysis.

TWO-DIMENSIONAL (2D) MIXED MODE FRACTURE CRITERIA

The fracture criteria should be based upon physical models accounting for damage processes of the material in front of the crack tip. However, since the exact description of these processes is difficult, the problems are usually treated within the framework of LEFM by using representative values such as stress components or specific strain energy specified at some finite distance from the crack or sharp notch tip. This characteristic distance specifying the core region affected by damage and plastic deformation is an unknown parameter to be specified experimentally or analytically.

The first fracture criteria related to the angled crack problem and the orientation of crack growth used the simplest assumption of the core region bounded by a circle of radius r_C from the crack tip. The criteria such as: maximum circumferential tensile stress (MTS) [1], minimum strain energy density (SED) [2], maximum energy release rate [3, 4] (MERR) and local symmetry [5] (LS), crack extension force criterion (CEF) [6], maximum tangential strain criterion (MTSN) [7], maximal stress triaxiality criterion (M_t-criterion) [8] became popular and were analyzed in the literature.

However, there exists the possibility to improve accuracy of the proposed fracture criteria by including the *T*-stress effect into the criterion. By adding the non-singular terms to singular stress, the value of *r* specifying the core region becomes essential. There have been numerous studies of extended fracture criteria accounting for *T*-stress, starting from the analysis of Wiliams and Ewing [9] related to MTS-criterion. The subsequent papers [10,11,12,13,14] demonstrated that the crack growth orientation depends on the radius *r* and better agreement with experiment can be attained by assuming the value of r_C to depend on the orientation angle θ.

A simple extension can be obtained by assuming the process zone to coincide with the localized plastic zone at the crack tip. This idea was applied in *T*-criterion [15], modifying the earlier SED-criterion. The specific stress and strain energy *T* is split into distortional T_D and hydrostatic portions T_V. Assuming the distortional energy to correspond to plastic flow and the hydrostatic stress energy to decohesion and fracture, the *T*-criterion postulates that the crack propagates along the direction corresponding to a maximum of total specific stress energy on the perimeter of varying radius $r = r_C(\theta)$ specified by the condition of constant distortional energy at the yield point. This criterion is formulated for the varying core region radius. In the case of brittle materials it tends to the SED criterion as the size of plastic zone is very small and its shape can be assumed as circular. *W*-criterion **[**16**]** proposed that the crack growth angle is specified by the minimum value of *W*-factor defined as $W = r_p(\theta)/a$ where $r_p(\theta)$ is radius of plastic zone and *a* is the half crack length. The Huber-Mises yield condition has been applied. The *W*-criterion is based on an assumption of the minimum energy consumed during the fracture process in the plastic zone. Yan et al.[17] specified the plastic core region by applying a more general yield condition which for the special case is equivalent to the Huber-Mises yield condition.

However, in the vicinity of the crack tip we may distinguish the zone characterized by growth of microcracks induced by tensile microstress [18]. This damage is related to the hydrostatic stress energy density T_V. Basing on this assumption Mróz [19] proposed the *MK*-fracture criterion postulating that size of damage zone is specified by the condition $T_V = T_V^C$ and macrocrack propagation follows the direction of smallest plastic dissipation, that is corresponds to a minimum value of the distortional stress energy T_D specified along the perimeter $T_V(r,\theta) = T_V^C = \text{const}$, thus

$$\left.\frac{T_V}{T_D}\right|_{\max} \to \theta_{pr} \quad \text{at} \quad T_V = T_V^C = \text{const.} \to \quad T_D\left(r(T_V^c,\theta)\right)\Big|_{\min} \to \theta_{pr}, \tag{1}$$

where

$$r(T_V^C,\theta,\alpha) = r_V\big|_{T_V=\text{const}} = \frac{2}{\pi}\left[\frac{K_I\cos\frac{\theta}{2} - K_{II}\sin\frac{\theta}{2}}{\sqrt{T_V^C\frac{6E}{(1-\nu)(1+\nu^*)^2}} - T(\alpha)}\right]^2 \tag{2}$$

and $\nu^* = 0$ for plane stress, $\nu^* = \nu$ for plane strain cases. Assume now, that the critical state is reached on the radius $r_C = \text{const}$. Assume that for a mixed mode loading the critical value of r_C is specified by the relation

$$r_C = \cos\gamma\, r_{CI} + \sin\gamma\, r_{CII} \tag{3}$$

where

$$\tan\gamma = \frac{K_{II}/K_{IIC}}{K_I/K_{IC}} \tag{4}$$

is a measure of mode mixity. Let us note that $r_C = r_{CI}$ for mode I ($\sin\gamma = 0$ and $\cos\gamma = 1$) and $r_C = r_{CII}$ for mode II ($\cos\gamma = 0$ and $\sin\gamma = 1$). The crack propagation criterion is now stated in the form

$$\left(K_I \cos\frac{\theta}{2} - K_{II}\sin\frac{\theta}{2}\right)^2 = \cos\gamma\left(K_{IC}\frac{\sigma_C - \sigma_\infty(1-k)\cos 2\alpha}{\sigma_C + \sigma_\infty(1-k)}\right)^2 + \\ + \sin\gamma\left(0.76\,K_{IIC}\frac{\sigma_C - \sigma_\infty(1-k)\cos 2\alpha}{\sigma_C}\right)^2. \tag{5}$$

THREE-DIMENSIONAL (3D) CRACKS AND FRACTURE CRITERIA.

Though there are numerous fracture criteria proposed for 2D stress states under I/II mixed mode conditions, only several 3D fracture criteria have been proposed and the related experimental work is limited. The first approach is based on the assumption that a new increment of fracture surface developing at the crack front is specified by locus of critical points and linear segments connecting these points to the crack front. The smooth crack surface is then generated. The other approach is based on the critical plane concept by specifying orientation of the critical plane element of a new fracture surface near the crack front. The critical plane approach allows for the rough crack surface evolution.

Crack growth modes.

Any growth of the plane crack surface which is located through the thickness of a plate, can obtained by superposition of three basic modes, Fig. 1. Two fundamental concepts can now be assumed: 1) the new crack growing surface is smooth and continuous at the edge of existing pre-crack, 2) the new crack surface is composed of facets of modes I, II and III oriented according to local critical state conditions. The crack surface is composed of the pattern of facets and its evolution is governed by geometric and mechanical characteristic of the element.

We shall refer to the first case as *smooth crack surface models (Fig. 2)* and to the second as *rough crack surface models (Fig. 3).*

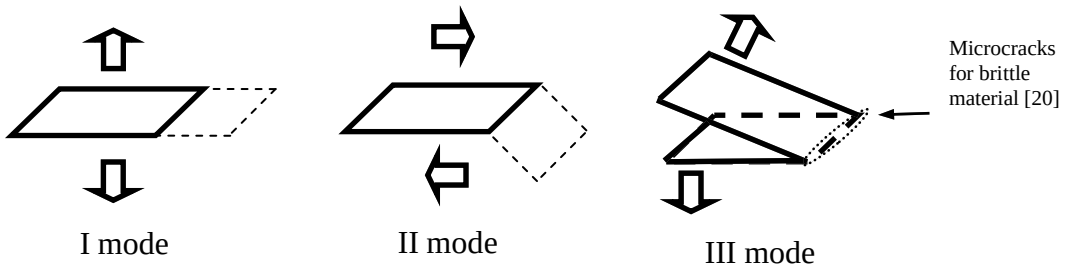

Fig. 1. Modes of plane crack edge growth.

To discuss these two approaches, consider the 3D square plane crack, within the 3D element. It can be expected that new crack surface may grow from each edge. However, satisfying the continuity conditions the new crack surface may evolve in mode I or II or in combined mode I+II. But the mode III loading and the associated crack facets generated locally by the K_{Imax} condition violate the continuity at the existing crack edge. Thus the mode III loading may induce the rough crack surface combined with facets developed in mode II, Fig. 3. In fact, brittle materials exhibit rough crack surface in mode III composed of facets of different modes, cf. [20, 21]. In ductile materials the shear band evolution may affect the crack roughness due localized plastic deformation and damage growth. In fact Dyskin and Salganik [22] analyzed 3D cracks in compression and showed that 3D crack growth can result in a more complicated growth mechanism than 2D. They investigated possible mechanism of wing crack growth induced also by rough crack surface and associated dilatancy effect [23].

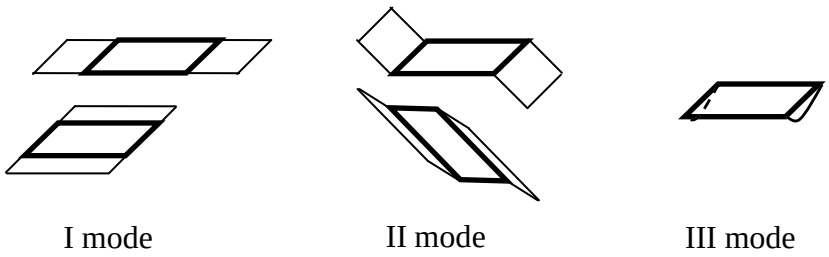

Fig. 2. Pure modes of smooth crack tip deformation.

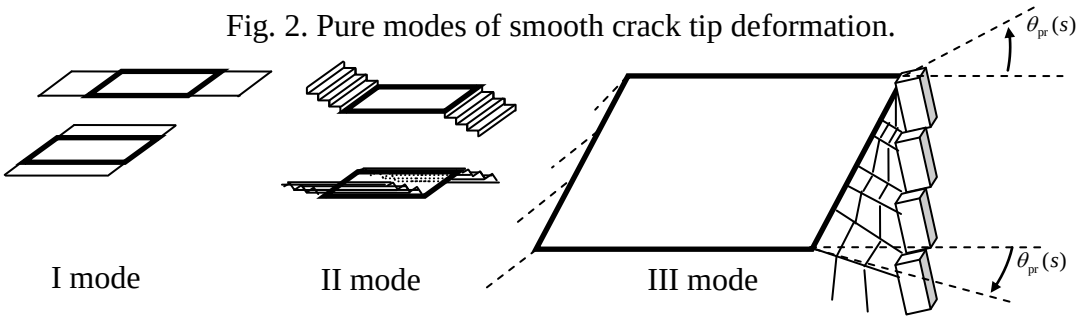

Fig. 3. Pure modes of rough 3D crack tip deformation.

A more general case of the 3D crack is the elliptic crack, which was analyzed in uniaxial compression tests by Adams and Sines [24] on PMMA samples. They showed that crack growth generally occurs in wing mode, but in addition at the lateral parts of crack edge a number of microcracks are developed. This can be interpreted as the mode III microcracks in brittle materials, cf. Figure 4. The extensively investigated 3D elliptical cracks embedded in brittle material under compression loading have also been analyzed by Dyskin et al [25,26].

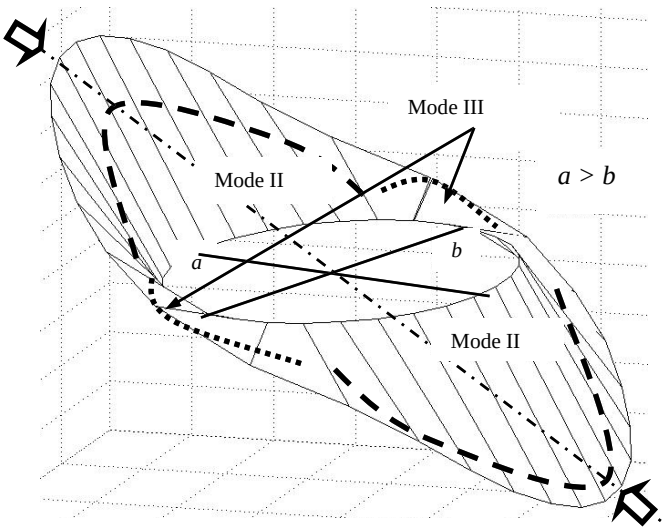

Fig. 4. 3D elliptic crack growth in compression.

Rough (dilatant) crack models

The effect of crack surface contact and asperity interaction is essential for modes II and III loading. In fact, the growth of precrack generated in mode I and next subjected to shear is associated with evolution of roughness pattern due to process of microcracking and associated inclined facets in mode I with subsequent connecting microcracks, cf. Pook [27]. The interface sliding along formed asperities induced mode I stress and crack dilatancy. Crack tip shielding then occurs due to frictional resistance to sliding and asperity interaction. The cases of closed or partially closed cracks subjected to shear and exhibiting contact shielding are numerous and occur, for instance, in compression or shear induced fracture of rocks or ceramic materials, rolling contact induced sub-surface fatigue cracks, mixed mode fatigue crack growth, etc. The referenced papers [21,28-35] contain both analytical and experimental studies of asperity interaction modes, specification of the effective SIFs and prediction of crack growth rates. The assumption of the contact interface interaction at the crack front or at the whole cracked interface provides different modelling effects. The detailed review of literature is not presented here. A simplified model of a closed crack interface will only be discussed in the following.

Consider a crack surface in a form of wedge shaped asperities, inclined at the angle $\gamma^z \in (0, \pi/2)$ to the nominal crack plane, Fig. 5.

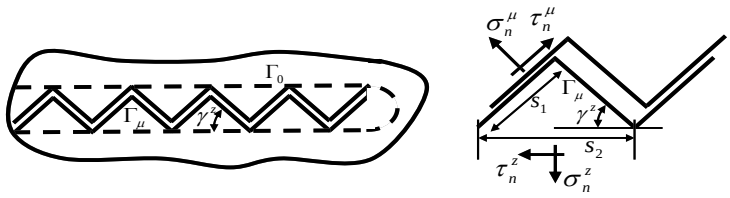

Fig. 5. Crack with wedge – shaped asperities and microstresses acting on asperities facet Γ_μ and stress acting on the nominal crack plane segment Γ_0.

Denote the local stresses acting on wedge flanks Γ_μ by σ_n^μ and τ_n^μ, so that the local friction condition on Γ_μ is

$$\tau_n^\mu = \eta^\mu \sigma_n^\mu = \tan\gamma^\mu \sigma_n^\mu \tag{6}$$

where η^μ is the local friction coefficient and γ^μ is the friction angle. The stress σ_n^z and τ_n^z acting on the nominal crack segment are expressed from the equilibrium equations for a single asperity, thus

$$\sigma_n^z = \sigma_n^\mu \frac{s_1}{s_2}(\cos\gamma^z - \eta^\mu \sin\gamma^z), \qquad \tau_n^z = \tau_n^\mu \frac{s_1}{s_2}(\sin\gamma^z + \eta^\mu \cos\gamma^z) \tag{7}$$

where s_1 denotes the wedge flank length and s_2 is the asperity length within the plane Γ_0. The conditions on the nominal plane Γ_0 can be expressed as follows

$$u_\vartheta = \pm|u_r|\tan\gamma^z, \qquad \tau_n^z = \sigma_n^z \tan(\gamma^z + \gamma^\mu), \quad \vartheta = \pm\pi \tag{8}$$

These conditions can be expressed in terms of the asymptotic fields with neglect of *T*-stress. Denoting by $K_{\mathrm{I}}^d, K_{\mathrm{II}}^d$ the effective SIFs for the dilatation crack model and by $K_{\mathrm{I}}^\mu, K_{\mathrm{II}}^\mu$ the SIFs resulting from the stress on the wedge asperity flanks Γ_μ, we obtain

$$K_{\mathrm{I}}^d = \left|K_{\mathrm{II}}^d\right| \tan\gamma^z, \qquad \left|K_{\mathrm{II}}^\mu\right| = K_{\mathrm{I}}^\mu \tan(\gamma^z + \gamma^\mu), \tag{9}$$

Denote by $K_{\mathrm{I}}, K_{\mathrm{II}}$ the SIFs for a smooth and plane crack. Applying the superposition principle for the external loading σ, τ and the wedge asperity loading σ_n^z, τ_n^z, the effective SIFs are

$$\begin{aligned} K_{\mathrm{I}}^d &= K_{\mathrm{I}} + K_{\mathrm{I}}^\mu = \frac{\sin\gamma^z}{\cos\gamma^\mu}(K_{\mathrm{I}} \sin(\gamma^z + \gamma^\mu) + \left|K_{\mathrm{II}}\right| \cos(\gamma^z + \gamma^\mu)), \\ \left|K_{\mathrm{II}}^d\right| &= K_{\mathrm{II}} + K_{\mathrm{II}}^\mu = \frac{\cos\gamma^z}{\sin\gamma^\mu}(K_{\mathrm{I}} \sin(\gamma^z + \gamma^\mu) + \left|K_{\mathrm{II}}\right| \cos(\gamma^z + \gamma^\mu)). \end{aligned} \tag{10}$$

These relations are valid when the contact occurs on Γ_μ, thus

$$-K_{\mathrm{I}} \tan(\gamma^z + \gamma^\mu) \le \left|K_{\mathrm{II}}\right| \ge K_{\mathrm{I}} \cot(\gamma^z). \tag{11}$$

These inequalities specify the sliding domain B, Fig. 6. When $\left|K_{\mathrm{II}}\right| < K_{\mathrm{I}} \cot(\gamma^z)$, the crack opening occurs, and the

domain A in Fig. 6 is specified. When $|K_{\mathrm{II}}| < -K_{\mathrm{I}}\ \tan(\gamma^z + \gamma^\mu)$, there is no slip at the contact interface and contact locking occurs.

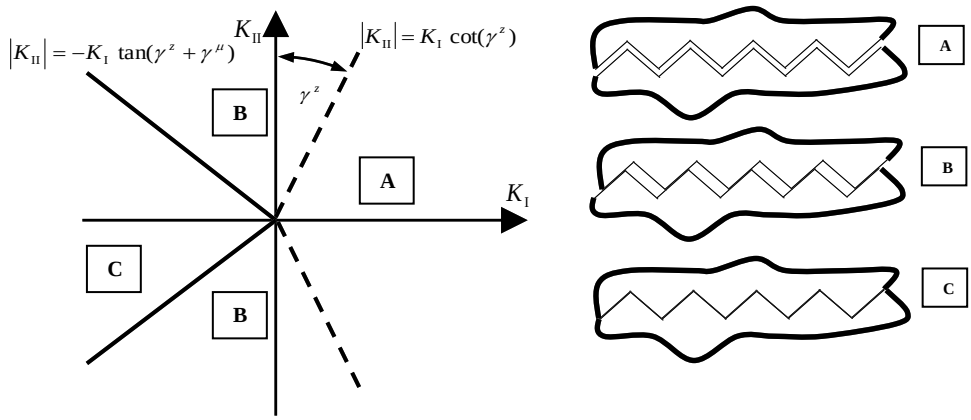

Fig. 6. Domain of crack loading for dilatant crack model: open model (A), slip and contact interface (B) and closed crack (C).

Smooth crack models

The stress analysis at the elliptical crack front was presented by Sih et al [36-38]. Firstly in [36,37] it was shown that the three dimensional stress state in a certain plane is identical to the two-dimensional case. However the stress intensity factor in general depends upon the curvature of the crack edge for three-dimensional problems. The same applies to the displacement field. In the subsequent paper Hartranft and Sih [39] provided the local singular 3D stress field at the crack front for small scale yielding. Using the singular stress components, Sih and Cha [40] extended the S-criterion to 3D by specifying the strain energy density near the crack front as follows

$$\frac{\mathrm{d}W}{\mathrm{d}V} = \frac{1}{r}\frac{S(\theta, s)}{\cos\phi} + O(1), \tag{12}$$

Similarly, as in the plane case, a minimum of the strain energy density factor S is searched on a sphere describing by r, ϕ, θ and centered at each point, s on the crack front [40, 41]. The crack growth occurs when S=$S_{\min}$ reaches critical value, S_{C}, and the size of r_{C} along a three-dimensional crack front is assumed to vary such that $S_{\min}(\theta, s)/r_C(s) = (dW/dV)_{\mathrm{cr}}$ remains constant. The continuous formulation $S(\theta)/\cos\phi$ exhibits a local minimum at (θ_0, ϕ_0) in the region $(-\pi \le \theta \le \pi), (-\pi/2 \le \phi \le \pi/2)$, provided $S(\theta, \phi) \ge S(\theta_0, \phi_0)$. It should be noted that $S(\theta)/\cos\phi$ attains a local minimum always in the normal plane to the crack front, so $\phi = 0$ in our case and direction of the crack growth does not depend on K_{III}. So, a minimum of S is searched on a circle centered at each point on the crack front. However, as this radius does not affect the value of S-factor, then $r_C(s) = S_{\min}(\theta_{\mathrm{pr}}, s)/(dW/dV)_{\mathrm{cr}}$ and generates the initial segment of the fracture surface.

The extension of stress triaxiality condition (M_t-criterion) to 3D cases was presented by Kong et al. [8]. Introducing the stress triaxiality parameter

$$M = \frac{\sigma_H}{\sigma_{EQ}} = \frac{F_1(\theta)}{F_2(\theta)} \tag{13}$$

The value of the ratio M is maximized with respect to the angle θ, as it does not depend on ϕ. The optimal orientation segments on the existing crack front then generate a new incremental crack surface and its size is specified by setting the critical value of $K_{\mathrm{I}} = K_{\mathrm{IC}}$ or of the effective SIF measure.

In a similar way the MK-criterion can be extended to 3D problems in the following form

$$\begin{aligned} T_{\mathrm{V}} &= \frac{1-2\nu}{6E}(\sigma_n + \sigma_z + \sigma_t), \\ T_{\mathrm{D}} &= \frac{1+\nu}{6E}((\sigma_t - \sigma_z)^2 + (\sigma_z - \sigma_n)^2 + (\sigma_n - \sigma_t)^2 + 6(\sigma_{nz}^2 + \sigma_{nt}^2 + \sigma_{zt}^2)), \end{aligned} \tag{14}$$

then

$$r_{\mathrm{V}}(\sigma_C, \theta, \alpha) = r_{\mathrm{V}}\big|_{T_{\mathrm{V}}=\mathrm{const}} = \frac{2}{\pi}\left[\frac{K_{\mathrm{I}}\cos\frac{\theta}{2}(1+\nu) - K_{\mathrm{II}}\sin\frac{\theta}{2}(1+\nu)}{\sigma_C}\right]^2. \tag{15}$$

The results of applied MK-criterion to the 3D problem of growth of elliptical crack under tension loading condition are presented in Figure 7. The size of the crack wings is calculated using Eq. (15).

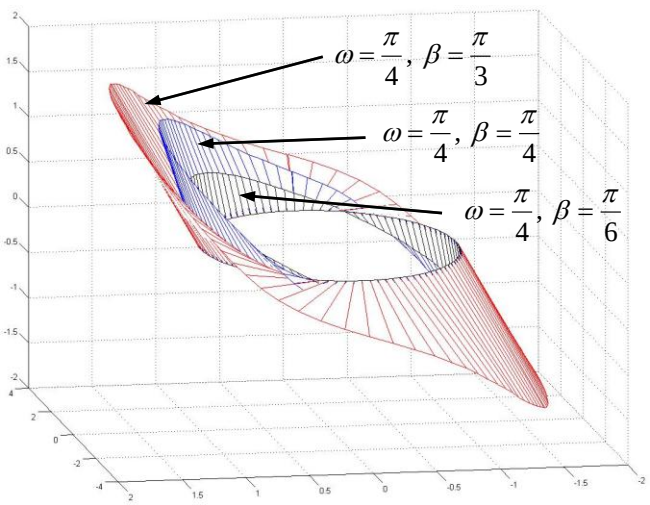

Fig. 7. 3D elliptical smooth crack growth based on the MK-criterion.

Critical plane criteria

Let us now present an alternative formulation of crack growth criteria based on the concept of critical plane. Such criteria are expressed in terms of traction or strain

components on the materials plane element. The unit vector $\bar{\mathbf{n}}$ specifies the orientation of plane. A general critical plane condition can be formulated as follows

$$F = \max_{\mathbf{n}} f(\sigma_n, \tau_n, \varepsilon_n, \gamma_n) - f_{\mathrm{C}}^* = 0 \tag{16}$$

where f_{C}^* represents the critical value reached by the failure condition generally depending on both stress and strain components associated with the respective planes. The comprehensive review was recently presented by Karolczuk and Macha [42].

In this section, the local critical plane models will be extended by introducing non-local failure criteria applicable to both regular and singular stress regimes and also for monotonic and cyclic loading cases.

Consider an arbitrary physical plane Δ and the local coordinate system (ξ_1, ξ_2, ξ_3), Fig. 8. In the global coordinate system (x_1, x_2, x_3) the origin of the local system is specified by the position vector $\mathbf{x}_0(x_{01}, x_{02}, x_{03})$ and the unit normal vector $\mathbf{n}(n_1, n_2, n_3)$ specifies the plane orientation, where $n_i = \cos(\xi_3, x_i)$.

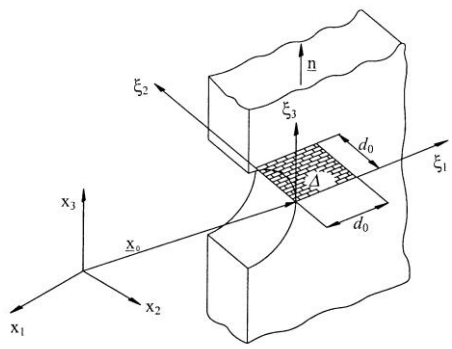

Fig. 8. The 3D system in R-criterion.

The resulting shear stress and strain in the plane Δ are expressed as follows: $\tau_n = (\tau_{n1}^2 + \tau_{n2}^2)^{1/2}$, $\gamma_n = (\gamma_{n1}^2 + \gamma_{n2}^2)^{1/2}$. Assume that crack initiation and propagation process depends on the contact stress and strain components and also on the damage accumulation on the physical plane. Consider an elliptical condition for $\sigma_n > 0$ and the Coulomb condition for $\sigma_n \le 0$, thus

$$F = R_\sigma\left(\frac{\sigma_n}{\sigma_c}, \frac{\tau_n}{\tau_c}\right) - 1 = \max_{\mathbf{n}} \left\{ \begin{array}{ll} \left[\left(\frac{\sigma_n}{\sigma_c}\right)^2 + \left(\frac{\tau_n}{\tau_c}\right)^2\right]^{1/2} - 1, & \sigma_n > 0, \\ \frac{1}{\tau_c}(|\tau_n| + \sigma_n \tan\varphi) - 1, & \sigma_n < 0, \end{array} \right\} \tag{17}$$

where σ_c, τ_c denote the failure stress of material in tension and shear. For large stress gradients or singular stress regimes such as those occurring at vertices of wedge shaped notches, the non-local stress failure conditions is applied by averaging the failure stress function over an area $d_0 \times d_0$, thus

$$\overline{F} = \overline{R}_\sigma - 1 = \max_{(\mathbf{n},\mathbf{x}_0)}\left[\frac{1}{d_0^2}\int_0^{d_0}\int_0^{d_0} R_\sigma \mathrm{d}\xi_1 \mathrm{d}\xi_2\right] - 1 = 0. \tag{18}$$

The size parameter d_0 representing the size of damage zone can be specified by requiring the non-local conditions (18) to be equivalent to the Griffith condition in the case of tensile crack propagation. This provides

$$d_0 = \frac{2}{\pi}\left(\frac{K_{Ic}}{\sigma_c}\right)^2, \tag{19}$$

where K_{Ic} is the critical stress intensity factor in Mode I. The extensive application of the non-local failure criterion to monotonically loaded elements witch sharp notches and cracks was discussed by Seweryn and Mróz [43,44]. The application to fatigue crack initiation and growth was discussed in [45,46] by applying the non-local criterion with account for local damage growth.

The Fatigue Crack Growth.

The history of rate of crack growth modelling starts from the Paris law [47,48] The equation predicts the fatigue crack growth in one cycle for the case of small scale yielding in terms of the amplitude ΔK in mode I. In actuality, the rate of crack growth depends on many factors, such as mean and maximal stress, crack closure effect, mode mixity, etc. There have been numerous extensions of Paris equation to account for other effects. Tanaka [49] introduced the concept of the effective stress intensity factor ΔK_{eff} for mixed mode conditions. Another form of the ΔK_{eff} resulting from the MTS-criterion was proposed by Yan et al. [50] based on the MTS-criterion. There are also other parameters used to correlate fatigue crack growth under mixed mode loading. Sih and Barthelemy [51] used the strain energy density factors ΔS replacing ΔK in the Paris type equation. They compared the predicted crack path using the S parameter with experimental data [52] for specimen made of Ti-6Al-4V with inclined cracks cf. Table 1.

Table 1.

Initial crack length a_0 [mm]	Specimen A: $a_0 = 7.11$[mm]	Specimen B: $a_0 = 6.73$[mm]
$\alpha[^\circ]$	$\alpha = 30$	$\alpha = 43$
$\sigma_{\min}$ [MPa]	20.69	17.24
$\sigma_{\max}$ [MPa]	206.85	172.38

However, these predictions are unsatisfactory, especially for $\alpha = 30^\circ$. The other parameter used frequently to predict the crack growth rate, the crack tip opening displacement [53-55], also. The application of MK-fracture criterion to the case of cyclic loading was presented in [19]. This criterion predicts the crack growth orientation depending on the load level. For the stress cycle with stress level varying between $\sigma_{\min}$ and $\sigma_{\max}$, the crack growth initiation stress σ_{pr} was introduced and assumption that $\sigma_{\mathrm{pr}} = \sigma_{\mathrm{op}}$, where σ_{op} is the crack opening stress associated with crack closure effect

[56]. Then it is assumed that $\sigma_{\mathrm{pr}} = \sigma_{\min}$ if $\sigma_{\min} > \sigma_{\mathrm{op}}$. The following relation specifying the crack growth per one cycle was proposed in [19]:

$$\frac{\mathrm{d}a}{\mathrm{d}N} = C(\Delta(T_D \cdot r(T_V^{\mathrm{const}}))),^n \tag{20}$$

where r is length of decohesion zone along the crack growth direction and C, n are the fatigue parameters obtained from uniaxial tests ($\alpha = 90^\circ$). In the case Ti-6Al-4V alloys the fatigue parameters are: 3.5 and 1.712. The comparison of model predictions and experimental results are shown in Tables 2 and 3. The comparison with predictions of R-criterion is also presented in tables in the following form

$$\frac{\mathrm{d}a}{\mathrm{d}N} = C_1 \Delta \left[\sqrt{\left(\frac{\sigma_n}{\sigma_c}\right)^2 + \left(\frac{\tau_n}{\tau_c}\right)^2} \right]^{n_1} \qquad \sigma_n > 0, \tag{21}$$

where C_1, n_1 are the fatigue constants for the uniaxial test ($\alpha = 90^\circ$). In the case Ti-6Al-4V alloys the parameters are $1{,}26 \cdot 10^{-14}$ and 5.4 respectively [57]. In the uniaxial test equation (21) is equivalent to Paris equation.

RIGTH TIP. (Eq. 21)			RIGHT AND LEFT TIP. (Eq. 20)			RIGHT TIP (Experimental results from [52])		
$\sum a$	$\sum N$	**d*a*/d*N***	$\sum a$	$\sum N$	**d*a*/d*N***	$\sum a$	$\sum N$	**d*a*/d*N***
[10^{-3}m]	**cykle**	**[10a^{-7}m]**	**[10^{-3}m]**	**cykle**	**[10^{-7}m]**	**[10^{-3}m]**	**cykle**	**[10^{-7}m]**
0,945	3583	2,64	**0,945**	**1390**	6,77	**0,91**	**1390**	6,54
1,705	**5416**	4,15	**1,705**	**2430**	6,25	**1,70**	**2430**	7,59
…								
4,58	**8695**	13,83	**4,58**	**5 400**	12,14	**4,55**	**5 400**	12
…								
6,86	**9813**	24,89	**6,86**	**7 000**	18,38	**6,86**	**7 000**	18

Table 2. Mixed mode fatigue crack growth in titanium alloys for specimen A.

RIGTH TIP. (Eq. 21)			RIGHT AND LEFT TIP. (Eq. 20)			RIGHT TIP (Experimental results from [52])		
$\sum a$	$\sum N$	**d*a*/d*N***	***a***	***N***	**d*a*/d*N***	***a***	***N***	**d*a*/d*N***
[10^{-3}m]	**cykle**	**[10^{-7}m]**	**[10^{-3}m]**	**cykle**	**[10^{-7}m]**	**[10^{-3}m]**	**cykle**	**[10^{-7}m]**
0,86	3546	1,64	**0,86**	**2 954**	2,91	**0,30**	**4 660**	1,85
…								
3,575	**12862**	4,19	**3,575**	**9 804**	4,91	**3,00**	**11 490**	5,77
…								
4,435	**14462**	5,72	**4,435**	**11 268**	6,15	**3,87**	**13 000**	3,91
…								
6,9	**17436**	10,36	**6,9**	**14 319**	9,54	**6,33**	**15960**	10,92

Table 3. Mixed mode fatigue crack growth in titanium alloys for specimen B.

CONCLUSIONS.

The present review paper presents synthetically different criteria of crack growth for 2D and 3D cases. The criteria are based on the elastic singular stress distribution and *T*-stress component. The energy concepts and critical plane approaches are discussed and their predictions compared for several specific cases. In the case of modes II and III loading the concepts of critical crack surface is introduced with account for frictional slip and dilatancy effects. For 3D cracks, both smooth and rough crack surfaces can be generated at different point location at the crack front.

Acknowledgment. The results presented in this paper have been obtained within the project "KomCerMet" (contract no. POIG.01.03.01-14-013/08-00 with the Polish Ministry of Science and Higher Education) in the framework of the Operational Programme Innovative Economy 2007-2013.

REFERENCES

1. Erdogan, F., Sih, G.C. (1963) On the crack extension in plates under plane loading and transverse shear, *Journal of Basic Engineering*, **85**, 519-527.
2. Sih, G.C. (1973) Some basic problems in fracture mechanics and new concepts, *Engng Fracture Mechanics*, **5**, 365-377.
3. Hussain, M.A., Pu, S.L., Underwood, J.H. (1974) Strain energy release rate for a crack under combined mode I and mode II, *Fracture Analysis*, ASTM STP, **560**, 2-28.
4. Wu, C.H. (1978) Fracture under combined loads by maximum-energy-release-rate-criterion, *ASME J. Appl. Mech*., **45**, 553-558.
5. Goldstein, R.V., Salganik, R.L. (1974), Brittle fracture of solids with arbitrary cracks, *Int. J. Fracture*, **10**, 507-523.
6. Strifors, H.C. (1973) A generalized force measure of conditions at crack tips, *Int. J. Solids Struct.*, **10**, 1389–1404.
7. Chang, K.J. (1981) On the maximum strain criterion. A new approach to the angled crack problem, *Engineering Fracture Mechanics*, **14**, 107-124.
8. Kong, X.M., Schluter, N., Dahl, W. (1995) Effect of triaxial stress on mixed-mode fracture, *Engineering Fracture Mechanics*, **52**, 379-388.
9. Ewing, P.D., Williams, J.G. (1972) Fracture under Complex Stress – The Angled Crack Problem, *International Journal of Fracture Mechanics*, **8**, 441-446.
10. Wu, X., Li, X. (1989) Analysis and modification of fracture criteria for mixed-mode crack, *Engng Fracture Mechanics*, **34**, 55-64.
11. Maiti, S.K., Smith, R.A. (1983) Comparison of the criteria for mixed mode brittle fracture based on the preinstability stress-strain field, part I: slit and elliptical cracks under uniaxial tensile loading, *Int. J. Fracture*, **23**, 281-295.

12. Wong, A.K. (1987) On the application of the strain energy density theoty in predicting crack initiation and angle of growth, *Engineering Fracture Mechanics*, **27**, 157-170.
13. Maiti, S.K., Smith, R.A. (1984) Criteria for brittle fracture in biaxial tension, Engineering Fracture Mechanics, **19**, 793-804.
14. Swedlow, J.L. (1976) Criteria for growth of the angled crack, In: *Cracks and fracture*, ASTM STP 601, 506-521.
15. Theocaris, P.S., Andrianopoulos, N.P. (1982) The Mises elastic-plastic boundary as the core region in fracture criteria, *Engineering Fracture Mechanics*, **16**, 425–432.
16. Wasiluk, B., Golos, K. (2000) Prediction of crack growth direction under plane stress for mixed-mode I and II loading, *Fatigue Fracture Engng Mater Structure*, **23**, 381-386.
17. Yan, X., Zhang, Z., Du, S. (1992) Mixed-mode fracture criteria for the materials with the different yield strength in tension and compression, *Engineering Fracture Mechanics*, **42**, 109-116.
18. Williams, J.G. (1984) *Fracture mechanics of polymers*, Ellis Horwood, Chichester.
19. Mróz K.P. (2008). Fatigue cracks growth in the bimaterial system. The mathematical model and numerical solution, Ph.D. thesis IPPT PAN (IFTR PAS), Warsaw, (in Polish).
20. Knauss, W.G. (1970) An observation of crack propagation in anti-plane shear, *Int. J. Fracture*, **1**, 183-185.
21. Tschegg, E.K., Suresh, S. (1988) Mode III fracture of 4340 steel: effects of tempering temperature and fracture surface interference, *Metall. Trans. A*, **19A**, 3035-3043.
22. Dyskin, A.V., Salganik, R.L. (1987) Model of dilatancy of brittle materials with cracks under compession, *Mech. Solids*, **22**, 165-173.
23. Brace, W.F., Paulding, B.W., Scholtz, C. (1966) Dilatancy in the fracture of crystalline rocks, *J. Geophys. Res.*, **71**, 3939-3953.
24. Adams, M., Sines, G. (1978) Crack extension from flaws in brittle material subjected to compression, *Tectonophysics*, **49**, 97-118.
25. Dyskin, A.V., Germanovich, L.N., Ustinow, K.B. (1999) A 3-D model of wing crack growth and interaction, *Engineering Fracture Mechanics*, **63**, 81-110.
26. Dyskin, A.V., Sahouryeh, E., Jewell, R.J., Joer, H., Ustinow, K.B. (2003) Influence of shape and locations of initial 3-D cracks on their growth in uniaxial compression, *Engineering Fracture Mechanics*, **70**, 2115-2136.
27. Pook, L.P. (2000) *Linear elastic fracture mechanics for engineers: theory and application*, WIT, Southampton.
28. Gross, T.S., Mendelsohn, D.A. (1989) Mode I stress intensity factors induced by fracture surface roughness under pure mode III loading: application to the effect of loading modes on stress corrosion crack growth, *Metall. Trans. A.*, **20A**, 1989-1999.

29. Tschegg, E.K. (1983) Sliding mode crack closure and Mode III fatigue crack growth in mild steel, *Acta Metall.*, **31**, 1323-1330.
30. Evans, A.G., Hutchinson, J.W. (1989) Effects of non-planarity on the mixed mode fracture resistance of biomaterial interfaces, *Acta Metall.*, **37**, 909-916.
31. Mendelsohn, D.A., Gross, T.S., Zhang, Y. (1995) Fracture surface interference in shear – I. A model based an experimental surface characterization, *Acta Metall. Mater.*, **43**, 893-900.
32. Gross, T.S., Zhang, Y., Watt, D.W. (1995) Fracture surface interference in shear – II. Experimental measurements of crack tip displacement field under mode II loading in 7075-T6Al, *Acta Metall. Mater.*, **43**, 901-906.
33. Mróz, Z., Seweryn, A. (1998) Non-local failure and damage evaluation rule: application to a dilatation crack model, *J. Phys. IV France*, **8**, 257-268.
34. Ballarini, R., Plesha, M.E. (1987) The effects of crack surface friction and roughness on crack tip stress fields, *Int. J. Fracture*, **34**, 195-207.
35. Pook, L.P. (2002) Crack Paths, WIT Press.
36. Kassir. M.K., Sih, G.C. (1974) Three dimensional crack problems. A new selection of crack problems in three dimensional elasticity, In: *Mechanics of Fracture II*, Sih G.C. (Ed.), Noordhoff.
37. Kassir. M.K., Sih, G.C. (1966) Three dimensional stress distribution around an elliptical crack under arbitrary loadings, *Journal of Applied Mechanics*, **33**, Trans. Asme, **88**, Series E, 601-611.
38. Hartranft, R.J., Sih, G.C. (1977) Stress singularity for a crack with an arbitrarily curved front, *Engng Fracture Mechanics*, **9**, 705-718.
39. Hartranft, R.J., Sih, G.C. (1969) The use of eigenfunction expansion in the general solution of three-dimensional crack problem, *Journal of Mathematics and Mechanics*, **19**, 123-138.
40. Sih, G.C., Cha, C.K. (1974) A fracture criterion for three-dimensional crack problems, *Eng. Fract. Mech.*, **6**, 699-723.
41. Zacharopoulos, D.A. (2004) Stability analysis of crack path using the strain energy density theory, *Theoretical and Applied Fracture Mechanics*, **41**, 327-337.
42. Karolczuk, A., Macha, E. (2005) A review of critical plane orientations in multiaxial fatigue failure criteria of metallic materials, *International Journal of Fracture*, **134**, 267–304.
43. Seweryn, A., Mróz, Z. (1995) A non-local stress failure conditions for structural elements under multiaxial loading, *Engineering Fracture Mechanics*, **51**, 955-973.
44. Seweryn A., Mróz, Z. (1998) On the criterion of damage evolution for variable maultiaxial stress state, *Int. J. Solids Structures*, **35**,1589-1616.
45. Seweryn, A., Poskrobko, S., Mróz, Z. (1997) Brittle fracture in plane elements with sharp notches under mixed-mode loading, *J. Eng. Mech.*, ASME, **123**, 535-543.
46. Mróz, Z., Seweryn, A., Tomczyk, A. (2005) Fatigue crack growth prediction accounting for the damage zone, *Fatigue Fract. Engng Mat. Struct.*, **28**, 61-71.

47. Paris, P. (1957) A note on the varies effecting the rate of crack growth due to cyclic loading, *The Boeing Company, Doc. No.D-17867*, Addendum N, September **12**.
48. Paris, P., Gomez, M.P., Anderson, W.E. (1961) A rational analytical theory of fatigue, *The Trend of Engineering*, **13**, 9–14.
49. Tanaka, K. (1974) Fatigue crack propagation from a crack inclined to the cyclic tensile axis, *Engng Fracture Mech.*, **6**, 493-507.
50. Yan, X., Du, S., Zhang, Z. (1992) Mixed mode fatigue crack growth prediction in biaxially stretched sheets, *Engineering Fracture Mechanics*, **43**, 471–475.
51. Sih, G.C., Barthelemy, B.M. (1980) Mixed mode fatigue crack growth predictions, *Engineering Fracture Mechanics*, **13**, 439–451.
52. Pustejovsky, M.A. (1979) Fatigue crack propagation in titanium under general in–plane loading – I: Experiments, *Eng. Fract. Mech.*, **11**, 9-15.
53. McEvily, A.J.(1979) *Metal Sci.*, 274–284.
54. Shademan, S., Soboyejo, A.B.O., Knott, J.F., Soboyejo, W.O. (2001) A physically– based model for the prediction of long fatigue crack growth in Ti-6Al-4V, *Materials Science and Engineering*, **A315**, 1-10.
55. Li, C. (1989) Vector CTD criterion applied to mixed mode fatigue crack growth, *Fatigue Fracture Engng Mater. Structures*, **12**, 59–65.
56. Elber, W. (1970) Fatigue crack closure under cyclic tension, *Eng. Fract. Mech.*, **2**, 37–45.
57. Langoy, M.A., Stock, S.R. (2001) Fatigue-crack growth in Ti-6Al-4V – 0.1Ru in air and seawater: Part I. Design of experiments, assessment, and crack-growth-rate curve, *Metallurgical and Materials Transaction A*, **32A**, 2297-2314.